Applied Catalysis B: Environmental 158–159 (2014) 85–90

Contents lists available at ScienceDirect

Applied Catalysis B: Environmental

journal homepage: www.elsevier.com/locate/apcatb

Reaction of $Cu(CN)_3^{2-}$ with H_2O_2 in water under alkaline conditions: Cyanide oxidation, Cu^+/Cu^{2+} catalysis and H_2O_2 decomposition

Fayuan Chen[a,b], Xu Zhao[a], Huijuan Liu[a], Jiuhui Qu[a,*]

[a] Key Laboratory of Aquatic Science and Technology, Research Center for Eco-Environmental Sciences, Chinese Academy of Sciences, Beijing 100085, PR China

[b] University of Chinese Academy of Sciences, Beijing 100085, PR China

ARTICLE INFO

Article history:
Received 26 November 2013
Received in revised form 3 March 2014
Accepted 7 April 2014
Available online 13 April 2014

Keywords:
Metal–cyanide complex
Hydrogen peroxide
Decomplexation
Fenton-like reaction

ABSTRACT

Cuprous cyanide is widely present in electroplating wastewater or metallurgical effluents. In the present study, the destruction of $Cu(CN)_3^{2-}$ with H_2O_2 in water under alkaline conditions was investigated. H_2O_2 oxidized the cyanide from $Cu(CN)_3^{2-}$ to cyanate with the formation of $Cu(CN)_2^-$ firstly. Following, the continuous oxidation of cyanide from $Cu(CN)_2^-$ and the attendant dissociation of $Cu(CN)_2^-$ led to progressive liberation of Cu^+. Transformation of Cu^+ to Cu^{2+} was confirmed afterward by X-ray photoelectron spectroscopy analysis. Meantime, the •OH signal was detected by electron spin resonance assay. It was concluded that Fenton-like reaction occurred between the liberated Cu^+ and H_2O_2. UV–vis spectra studies revealed the formation of superoxo-cupric complex between Cu^{2+} and H_2O_2 in alkaline conditions, which decomposed into Cu^{2+} species and O_2 finally. Thus, how to improve the utilization of H_2O_2 and enhance the destruction of $Cu(CN)_3^{2-}$ should be considered in the treatment of $Cu(CN)_3^{2-}$ wastewater.

1. Introduction

Cyanide is widely used in electroplating industry [1] and metallurgical process [2]. The cyanide and copper often occur in the effluents simultaneously; the cyanide species may exist as CN^-, $Cu(CN)_4^{3-}$, $Cu(CN)_3^{2-}$, and $Cu(CN)_2^-$ [3], which must be adequately treated before being allowed to discharge due to its high toxicity. Different techniques have been proposed for the treatment of cyanide-contaminated effluents. Electrochemical oxidation is generally suitable for removing concentrated cyanide solutions [4,5]. The plasma method [6] and biological treatment [7,8] could be used to remove cyanide with low loads from wastewaters. Photocatalysis is also effective for cyanide oxidation [9,10]. Nevertheless, the existence of co-contaminants in these aqueous wastes can cause inhibitory effects on the three processes [6,7,10]. Though wet oxidation is adequate for the treatment of wastewaters containing various cyanide species, energy requirements are quite high [11]. Ferrate oxidation is effective in removing free cyanide and metal complex cyanide [12,13]. But, it was limited owing to the instability of the chemical [14]. Ozonation of free cyanide or complexed cyanide is limited by low rate of ozone mass transfer into aqueous phase at high pH [15]. The most practiced method is alkaline chlorination, which has many disadvantages such as formation of toxic cyanogens chloride [16] and chloride disinfection by-products [17]. With respect to the method of adsorption, precipitation and ion-change, secondary treatment was generally needed [18–20].

H_2O_2 oxidation is particularly interesting because of it does not add any toxic pollutant. Oxidation of various species of cyanide in water by H_2O_2 has been investigated recently. It was reported that 90% of cyanide with the concentration of 100 mg/L was removed in 24 h with 88.2 mM H_2O_2 [21]; in the presence of pumice impregnated with copper, more than 90% of cyanide was removed in 1 h with 4.4 mM H_2O_2 [22]. By contrast, more than 90% of cyanide with the initial cyanide concentration of 260 mg/L was removed in 20 min at pH 11 with the initial molar ratio (H_2O_2/CN) of 1.0 in the presence of copper-impregnated activated carbon (AC-CuO) [23]. In addition, the oxidation of $Cu(CN)_3^{2-}$ and $Cu(CN)_2^-$ by H_2O_2 was investigated by Beattie et al. [24].

The above studies mainly focused on the oxidation of cyanide by H_2O_2. The reaction of $Cu(CN)_3^{2-}$ with H_2O_2 has received little attention, especially the reaction of Cu^+/Cu^{2+} with H_2O_2 in the process. In previous studies, the various reaction mechanisms between Cu^+/Cu^{2+} and H_2O_2 were reported. Eberhardt et al. investigated the reaction of Cu^+ with H_2O_2 by using fluorobenzene, anisole, and nitrobenzene as a probe for •OH and it was concluded that •OH was the major species resulting from the reaction [25]. In the presence of ethanol, 2-propanol and 2-butanol, it was found that $Cu–O_2H$ complex was formed stably between Cu^+ with H_2O_2 [26].

* Corresponding author. Tel.: +86 10 62849151; fax: +86 10 6292355.
E-mail address: jhqu@rcees.ac.cn (J. Qu).

http://dx.doi.org/10.1016/j.apcatb.2014.04.010
0926-3373/

The reaction of nanomolar concentration of Cu^+ with H_2O_2 was investigated in 2.0 mM $NaHCO_3$ and 0.7 M NaCl solutions at pH 8.0 [27]. Measurements of both the formation of the hydroxylated phthalhydrazide chemiluminescent product and the degradation of formate indicated that a higher oxidation state of copper, Cu^{3+} formed rather than •OH. The Cu^+ with ligand chloride even did not react with H_2O_2 at all in natural waters [28]. The reaction of Cu^+ with H_2O_2 is strongly dependent upon the ligand environment and the solution pH. As to the reaction of Cu^+ from $Cu(CN)_3^{2-}$ with H_2O_2 under alkaline conditions, there was no clear understanding up to date. In one way, •OH may be produced expectedly from H_2O_2 through Cu^+/Cu^{2+} catalysis; in another way, decomposition of H_2O_2 may occur in the presence of Cu^{2+}. These issues are concerned with whether H_2O_2 oxidation or advanced oxidation process based H_2O_2 is an efficient technology in practical application in treating $Cu(CN)_3^{2-}$ in water.

Thus, the reaction of $Cu(CN)_3^{2-}$ with H_2O_2 was investigated under alkaline conditions in this study to answer three particular questions: (a) whether the $Cu(CN)_3^{2-}$ is destroyed completely with H_2O_2? (b) Whether or not the catalytic reaction takes place between Cu^+/Cu^{2+} and H_2O_2? (c) Whether the H_2O_2 is inefficiently decomposed? Finally, a reaction process of $Cu(CN)_3^{2-}$ with H_2O_2 was proposed. Investigation of this process provides additional understanding not only in treating $Cu(CN)_3^{2-}$ wastewater with H_2O_2, but also in the redox reaction of Cu^+/Cu^{2+} species with H_2O_2.

2. Experimental

2.1. Chemicals

Sodium cyanide, cuprous cyanide, hydrogen peroxide (wt 30.0%), sodium hydroxide, perchloric acid, and potassium iodide were all purchased from Sinopharm chemical regent Co., Ltd. The reagent 5, 5-dimethyl-1-pyrroline-*N*-oxide (DMPO) was bought from Sigma Chemical Co. All chemicals were analytical grade. Deionized water was used for the preparation and dilution of solutions.

$Cu(CN)_3^{2-}$ were prepared by the addition of cuprous cyanide powder to cyanide solutions at a molar ratio of CN^- to Cu^+ (3.0:1.0 or 4.0:1.0) according to the procedure [29]. Cuprous cyanide species distribution was calculated with the program Visual MINTEQ 3.0. In the solutions, $Cu(CN)_3^{2-}$ is the predominant species at the ratio of 3.0:1.0 (Fig. S1(a)). Both the concentration of free cyanide and $Cu(CN)_3^{2-}$ are about 1.0 mM with the ratio of 4.0:1.0 (Fig. S1(b)), respectively.

2.2. Experiment procedures

The pH of cyanide solutions was maintained above 11.0 to avoid release of HCN gas [30]. The H_2O_2 deprotonated and existed as H_2O^- when the pH of solution was above 12.0 [31]. So, the pH of solutions was adjusted to 11.0 by reagent grade $HClO_4$ or NaOH in the experiments.

Stoichiometry studies were conducted by addition of various concentration of H_2O_2 into CN^-, $Cu(CN)_3^{2-}$, and CN^-, $Cu(CN)_3^{2-}$ co-existing solutions, respectively. The H_2O_2 concentrations ranged from 0 to 18.0 mM. The cyanide concentration was fixed at 3.0 mM in the CN^- and $Cu(CN)_3^{2-}$ solutions. The cyanide was fixed at 4.0 mM in CN^-, $Cu(CN)_3^{2-}$ co-existing system. The stoichiometry of the cyanide oxidation with H_2O_2 was examined by an analysis of the residual cyanide after complete reaction of H_2O_2 with CN^- or (and) $Cu(CN)_3^{2-}$. The residual cyanide concentration was analyzed after 72 h in the CN^- system, while after 12 h in the $Cu(CN)_3^{2-}$, and CN^-, $Cu(CN)_3^{2-}$ co-existing system. The stoichiometry of the Cu^+ oxidation with H_2O_2 was also examined by an analysis of the copper concentration after complete reaction. The samples for analysis of copper were filtrated firstly. Once Cu^+ was oxidized into Cu^{2+}, $Cu(OH)_2$ precipitation was generated at alkaline conditions, which can be removed by filtration. The copper in the filtrate was considered as cuprous complex.

Other experiments were performed in 0.5 L glass beaker and magnetic stirrer was used to keep the chemicals uniform. The beaker was covered with aluminum foil paper. Given concentration of H_2O_2 was added in the beaker. The samples were taken at different time intervals, and were distilled immediately after sufficient amount of potassium iodide was added to terminate reaction. The concentration of potassium iodide was kept in 1.2 times of initial H_2O_2 concentration.

2.3. Analytical procedures

The total cyanide concentration was determined by colorimetric method after distillation [32]. Cyanate concentration was determined by hydrolyzing to ammonia measured by Nesslerization method [32]. Concentrations of copper ions were measured using a 700 series inductively coupled plasma optical emission spectrometer (ICP–OES, Agilent Technology). H_2O_2 concentration was determined colorimetrically using potassium titanium oxalate solution at 400 nm [33]. The dissolved oxygen (DO) concentration was determined by an oxygen electrode (Model 97-08-99, Orion Research Inc., Beverly, MA).

ESR spectra were obtained using electron paramagnetic resonance spectrometer (ESP 300E, Bruker). The settings were centerfield, 3480.00 × G; microwave frequency, 9.79 GHz; power, 5.05 mW. For this study, all the ESR spectra were recorded in situ using DMPO as the radical scavenger. The amount of •OH was quantified according to the literatures [34,35], as described in the Supporting Information.

The samples were taken at different reaction times in the reaction process of $Cu(CN)_3^{2-}$ with H_2O_2. The potassium iodide solution with given concentration was added into the samples to terminate the reaction of $Cu(CN)_3^{2-}$ with H_2O_2. After that, the samples were treated by freeze–drying. The freeze-dried powder was characterized by X-ray photoelectron spectroscopy (XPS) and X-ray diffraction (XRD). XPS data were taken on an AXIS-Ultra instrument from Kratos using monochromatic Al *K*α radiation (225 W, 15 mA, 15 kV) and low-energy electron flooding for charge compensation. To compensate for surface charge effects, the binding energies were calibrated using the C1s hydrocarbon peak at 284.80 eV. XRD pattern of the samples after vacuum freeze-drying were recorded on a Scintag-XDS-2000 diffract meter with Cu *K*α radiation λ = 1.540598 Å. The generator voltage and tube current used were 40 kV and 40 mA, respectively.

3. Results and discussion

3.1. Destruction of $Cu(CN)_3^{2-}$ with H_2O_2

3.1.1. Stochiometries of free cyanide oxidation and $Cu(CN)_3^{2-}$ oxidation

First, the stoichiometries of free cyanide oxidation (3.0 mM) and $Cu(CN)_3^{2-}$ oxidation (1.0 mM) were performed with various concentration of H_2O_2 at pH 11.0. The stoichiometric relationship between cyanide and H_2O_2 is shown in Fig. 1. In the case of free cyanide (Fig. 1(a)), when the initial H_2O_2 concentration increases from 0 to 3.0 mM, cyanide concentration linearly decreases. The slope ($\Delta[CN^-]/\Delta[H_2O_2]$) of the line gives stoichiometry for the reaction as −0.97, which indicates a stoichiometric ratio of 1.0.

In the case of $Cu(CN)_3^{2-}$ (Fig. 1(b)), when the initial H_2O_2 concentration increases from 0 to 1.0 mM, cyanide concentration

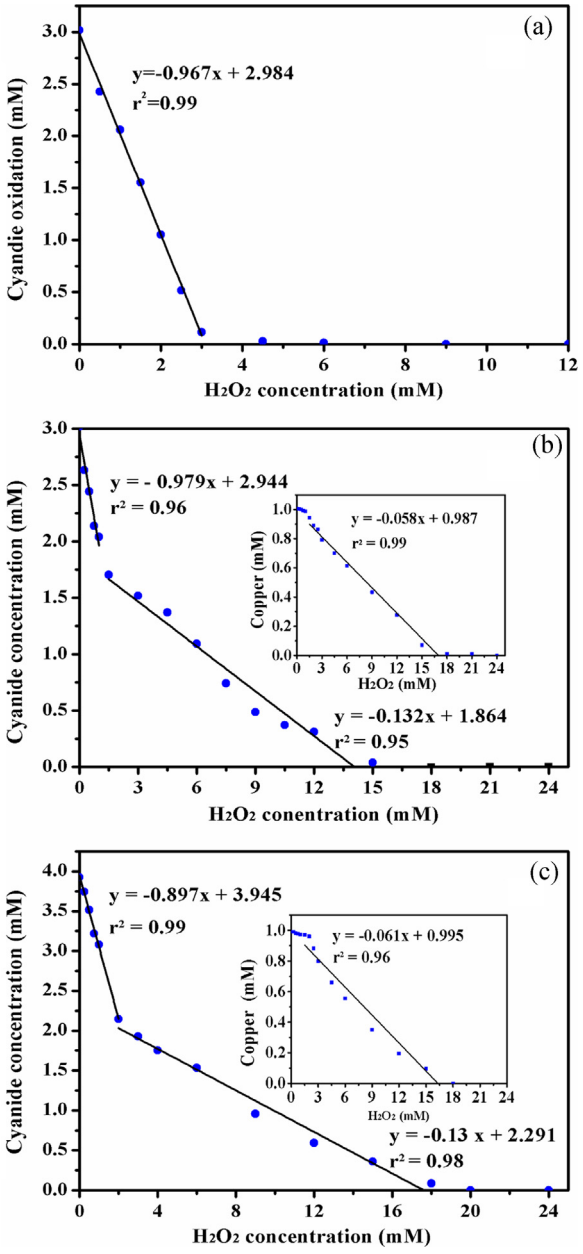

Fig. 1. Plots of residual cyanide concentration with initial H_2O_2 concentration: (a) CN^- (3.0 mM), (b) $Cu(CN)_3^{2-}$ (1.0 mM), (c) CN^- (1.0 mM) and $Cu(CN)_3^{2-}$ (1.0 mM) (in box, plots of soluble copper concentration with initial H_2O_2 concentration pH: 11, *T*: 25 °C).

linearly decreases, but the copper concentration in the filtrate nearly remains constant (Fig. 1(b) inbox). The slope of the line gives stoichiometry as −0.98. It is implied that the cyanide was oxidized by H_2O_2 at this phase. When the initial H_2O_2 concentration increases from 1.0 to 16.0 mM, cyanide concentration linearly decreases and the slope ($\Delta[CN^-]/\Delta[H_2O_2]$) of the line gives stoichiometry as −0.13, implying that the Cu^+ was also oxidized by H_2O_2 besides cyanide. The copper concentration in the filtrate linearly decreases and the slope ($\Delta[Cu]/\Delta[H_2O_2]$) of the line gives stoichiometry as −0.06. Thus, the value of $\Delta[CN^-]/\Delta[Cu]$ is near to 2.0, which was calculated from $\Delta[CN^-]/\Delta[H_2O_2]$ and $\Delta[Cu]/\Delta[H_2O_2]$. The relationship between cyanide concentration and copper concentration indirectly evidenced that $Cu(CN)_2^-$ was the predominant species until its complete disassociation. The Cu^+ was liberated progressively from $Cu(CN)_2^-$ as a result of continuous cyanide oxidation. The Cu^+ was oxidized subsequently.

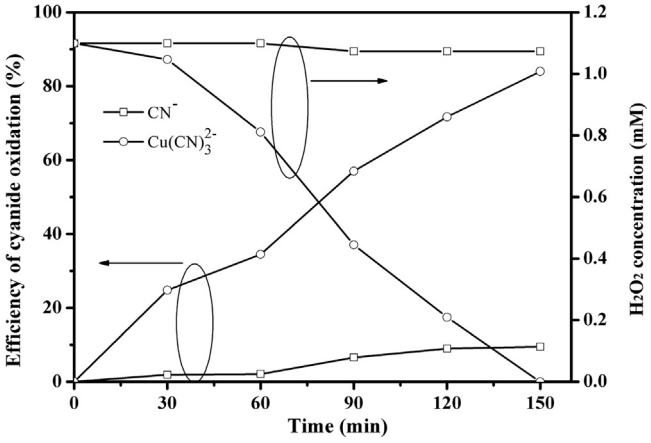

Fig. 2. Efficiency of cyanide oxidation in free cyanide and $Cu(CN)_3^{2-}$ oxidation process (CN^-: 3 mM, $Cu(CN)_3^{2-}$: 1.0 mM, H_2O_2: 1.0 mM, pH: 11, *T*: 25 °C).

The complete destruction of $Cu(CN)_2^-$ required a large amount of H_2O_2.

3.1.2. Stoichiometry of $Cu(CN)_3^{2-}$ oxidation in presence of free cyanide

The stoichiometry of $Cu(CN)_3^{2-}$ oxidation (1.0 mM) in the presence of free cyanide (1.0 mM) by H_2O_2 was also performed (Fig. 1(c)). When the initial H_2O_2 concentration increases from 0 to 2.0 mM, cyanide concentration linearly decreases, but the copper concentration in the filtrate nearly remains constant (Fig. 1(c) inbox). The slope of the line ($\Delta[CN^-]/\Delta[H_2O_2]$) gives stoichiometry as −0.90, indicating that oxidation of both complex cyanide and free cyanide occurred at this phase. When the initial H_2O_2 concentration increases from 2.0 to 18.0 mM, cyanide concentration linearly decreases and the slope of line ($\Delta[CN]/\Delta[H_2O_2]$) gives stoichiometry as −0.13. The copper concentration in the filtrate linearly decreases and the slope of line ($\Delta[Cu]/\Delta[H_2O_2]$) gives stoichiometry as −0.06. The value of $\Delta[CN^-]/\Delta[Cu]$ is found to be 2.0, which was calculated from $\Delta[CN^-]/\Delta[H_2O_2]$ and $\Delta[Cu]/\Delta[H_2O_2]$. These results show that the $Cu(CN)_2^-$ oxidation proceeded at this phase as previous illustrated.

The oxidation of $Cu(CN)_3^{2-}$ was much faster than oxidation of free cyanide with H_2O_2, which is further evident from various consumption of H_2O_2 over time in the oxidation of $Cu(CN)_3^{2-}$ and free cyanide (Fig. 2). These results suggest that the reactivity of $Cu(CN)_3^{2-}$ with H_2O_2 is more higher than free cyanide with H_2O_2. Thus, the reaction of free cyanide with $Cu(CN)_2^-$ formed $Cu(CN)_3^{2-}$ immediately, which was further oxidized into $Cu(CN)_2^-$. The conversion between $Cu(CN)_3^{2-}$ and $Cu(CN)_2^-$ proceeded continuously up to no free cyanide in the solution. A comparison of the reactivity of different metal cyanide complex ($Cd(CN)_4^{2-}$, $Zn(CN)_4^{2-}$, $Ni(CN)_4^{2-}$, $Cu(CN)_4^{3-}$) and free cyanide with Fe(VI) also indicated that $Cu(CN)_4^{3-}$ was the most reactive complex [13]. Copper(I) salts in general are relatively unstable and rapidly transfer an electro to form Cu^{2+} ion. Recent quantum calculations on cyanides and isocyanides of transition metals also suggested that metal–carbon bonds are involved rather than N-bonded cyanide complex [36].

3.1.3. Product of cyanide oxidation

To analyze the pathway of cyanide oxidation with H_2O_2, intermediates of cyanide oxidation were identified in the course of $Cu(CN)_3^{2-}$ oxidation. As shown in Fig. 3, the cyanate concentration increases with the decrease of cyanide concentration. In the present study, ammonia, nitrite and nitrate were not found. The sum of the cyanide concentration and cyanate concentration at different reaction times was found to be nearly equal to the initial cyanide

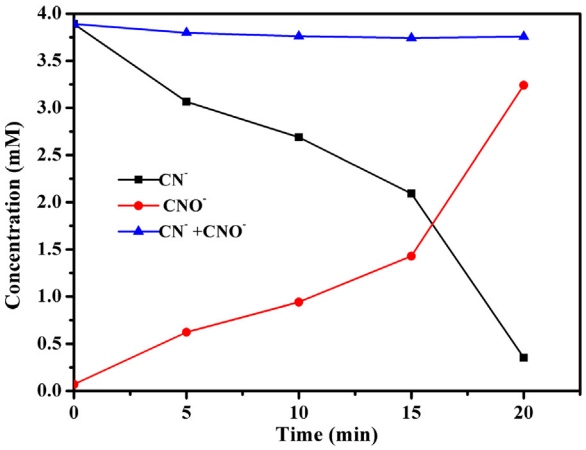

Fig. 3. Cyanide transformation during the process of $Cu(CN)_3^{2-}$ oxidation ($Cu(CN)_3^{2-}$: 1.0 mM, CN^-: 1.0 mM, H_2O_2: 12.0 mM, pH: 11, *T*: 25 °C).

concentration, indicating cyanate was the only oxidized product of cyanide in the experiment.

3.2. The catalytic reaction of Cu^+/Cu^{2+} with H_2O_2

3.2.1. H_2O_2 decay and its involved radicals with $Cu(CN)_3^{2-}$ oxidation

Herein, H_2O_2 decay and DO change over time during the course of $Cu(CN)_3^{2-}$ oxidation are shown in Fig. 4(a). A different variation trend of H_2O_2 decay and DO change with the reaction time was observed. Before 15 min, H_2O_2 concentration declines moderately and DO dose almost does not change. After that, H_2O_2 concentration declines steeply and DO dose goes up sharply. H_2O_2 is decomposed

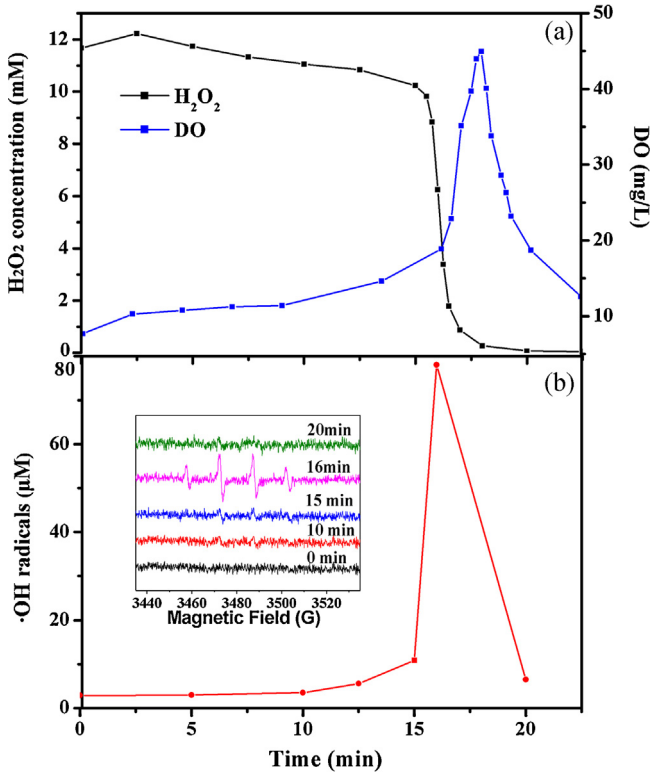

Fig. 4. (a) H_2O_2 decay and DO change during the process of $Cu(CN)_3^{2-}$ oxidation, (b) •OH change during the process of $Cu(CN)_3^{2-}$ oxidation, inset, ESR signal DMPO-•OH in aqueous dispersion during the process of $Cu(CN)_3^{2-}$ oxidation, ($Cu(CN)_3^{2-}$: 1.0 mM, CN^-: 1.0 mM, H_2O_2: 12.0 mM, pH: 11, *T*: 25 °C).

completely at 18 min. Correspondingly, DO reach the peak. It indicates that H_2O_2 was mainly decomposed into O_2 in this phase.

The formation of •OH in the course of $Cu(CN)_3^{2-}$ oxidation was also investigated by ESR spin-trap technique. The change of signal intensity at different reaction times is shown in Fig. 4(b). The characteristic four peaks of DMPO–•OH with intensity of 1:2:2:1 are clearly observed at 16 min, which confirms the generation of the •OH radicals [37], while the peaks disappear at 20 min. By contrast, the characteristic peaks of DMPO–•OH do not appear at 0, 5, 10, and 15 min. Meantime, the concentration of •OH at different reaction times was examined (Fig. 4(b), inset). Within 15 min, the •OH concentration is below 5.0 μM. At 16 min, the amount of •OH is determined to be 78.0 μM. By contrast, the •OH concentration is below 5.0 μM at 20 min. The production of •OH preceded the increase of DO, implying that Cu^+ oxidation occurred before the decomposition of H_2O_2 into O_2. The •OH trapping studies reveal that cyanide oxidation did not been retarded whatever bicarbonate or *t*-BuOH as scavenger (Fig. S2(a) and Fig. S2(b)). Therefore, the cyanide oxidation by •OH could be negligible in the experiment.

3.2.2. Transformation of copper species with $Cu(CN)_3^{2-}$ oxidation

In order to examine the transformation of Cu^+ to Cu^{2+} during the course of $Cu(CN)_3^{2-}$ destruction, XPS analysis and XRD measurements were conducted on the freeze-dried samples taken at different reaction times. As shown in Fig. 5, the peaks corresponding to Cu 2p3/2 at ca. 932.8 eV are observed for the samples at 0, 5, 10 and 15 min, which are in good agreement with the reported values for Cu^+ [38]. For the sample at 20 min, the peaks corresponding to the Cu 2p3/2 are observed at 934.4 eV for Cu^{2+}, Cu^{2+} ion could also be distinguished by the appearance of a shake-up satellite line at ca. 941.2–943.7 eV [39]. It is suggested that the Cu^+ was oxidized into Cu^{2+} after 15 min. As shown in Fig. 6, the XRD patterns of the samples at 0 and 10 min exhibit the features of $Na_2Cu(CN)_3$ (JCPDS 70-1064) and NaCN (JCPDS 04-0665). The diffraction peak of NaCNO (JCPDS 44-0770) appears in the samples taken at 10, 15 and 20 min, while the peak of $Na_2Cu(CN)_3$ and NaCN gradually faded away. It indicates that $Cu(CN)_3^{2-}$ was destructed with the formation of CNO^-. For the sample at 20 min, nearly no diffraction peak for the crystalline phases of copper oxides (JCPDS 89-2529) is observed due to the content below XRD detection limit presumably. It is inferred that $Cu(OH)_2$ was the predominant species.

In addition, the reaction of Cu^+ with H_2O_2 may produce Cu^{3+} except for Cu^{2+}. The dissociation of Cu^{3+} produced •OH in acidic solutions [27]. However, the rate of formation of •OH from the dissociation of Cu^{3+} was extremely slow at pH 8.0 [27], and the •OH was not formed in alkaline solutions [25]. Since our experiments were carried out in alkaline solutions (at pH 11.0), it was concluded that the •OH are formed via a Fenton-like reaction rather than the dissociation of Cu^{3+}.

3.3. The H_2O_2 decomposition

UV–vis spectrum of the $Cu(CN)_3^{2-}$ solution with the addition of H_2O_2 was recorded at various times. At 16 min, the absorbance spectrum of the solution appears in the visible light region, which disappears at 20 min (Fig. 7(a)). The Cu^+ has been oxidized into Cu^{2+} after 15 min according to XPS analysis. It has been reported that the reaction between H_2O_2 and Cu^{2+} in strongly alkaline medium led to the formation of the species with the absorbance in the region of 340–700 nm [40]. To verify the formation of the species in the experiment, spectrophotometric studies about the reaction of Cu^{2+} with H_2O_2 were conducted at various pH and with various H_2O_2 concentrations at pH 11. The absorbance in the region of 340-700 nm is observed after the addition of H_2O_2 to $CuClO_4$ solutions as the pH value is higher than 7.0, which increases with the increase of pH value (Fig. 7(b)). The absorbance intensity also increases with

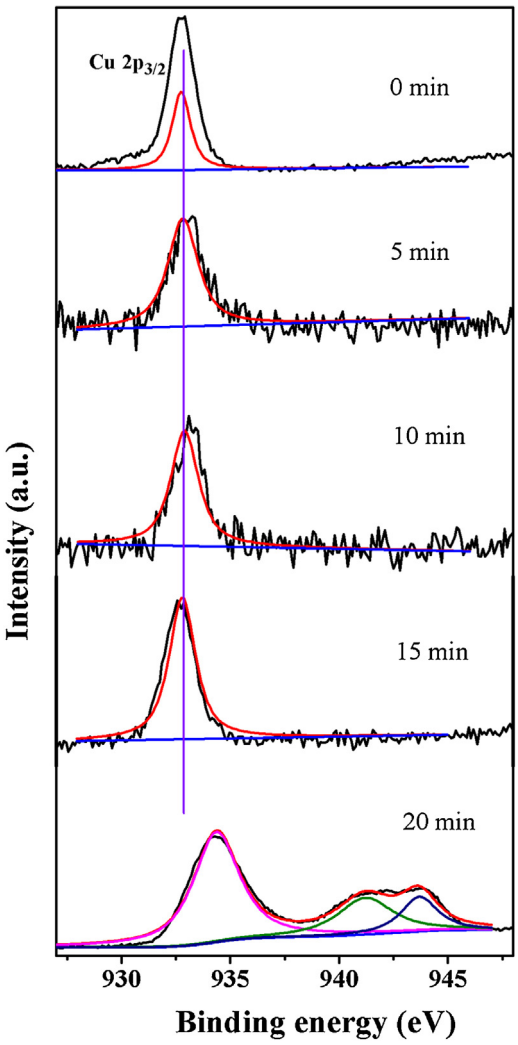

Fig. 5. XPS spectra of the freeze-dried samples collected at different time in the process of $Cu(CN)_3^{2-}$ oxidation by H_2O_2 ($Cu(CN)_3^{2-}$: 1.0 mM, CN^-: 1.0 mM, H_2O_2: 12.0 mM, pH: 11, *T*: 25 °C).

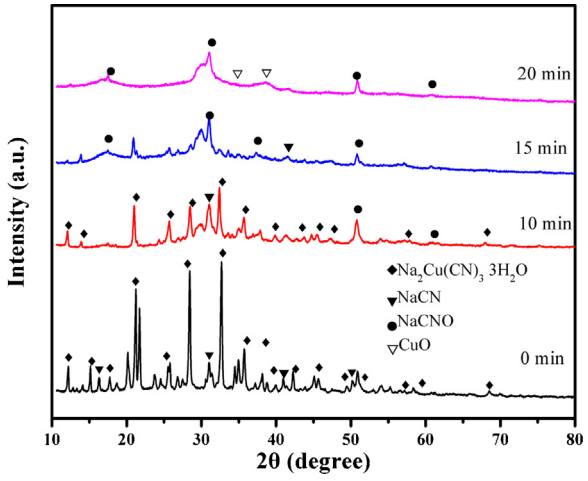

Fig. 6. XRD patterns of the freeze-dried samples collected at different time in the process of $Cu(CN)_3^{2-}$ oxidation by H_2O_2 ($Cu(CN)_3^{2-}$: 1.0 mM, CN^-: 1.0 mM, H_2O_2: 12.0 mM, pH: 11, *T*: 25 °C).

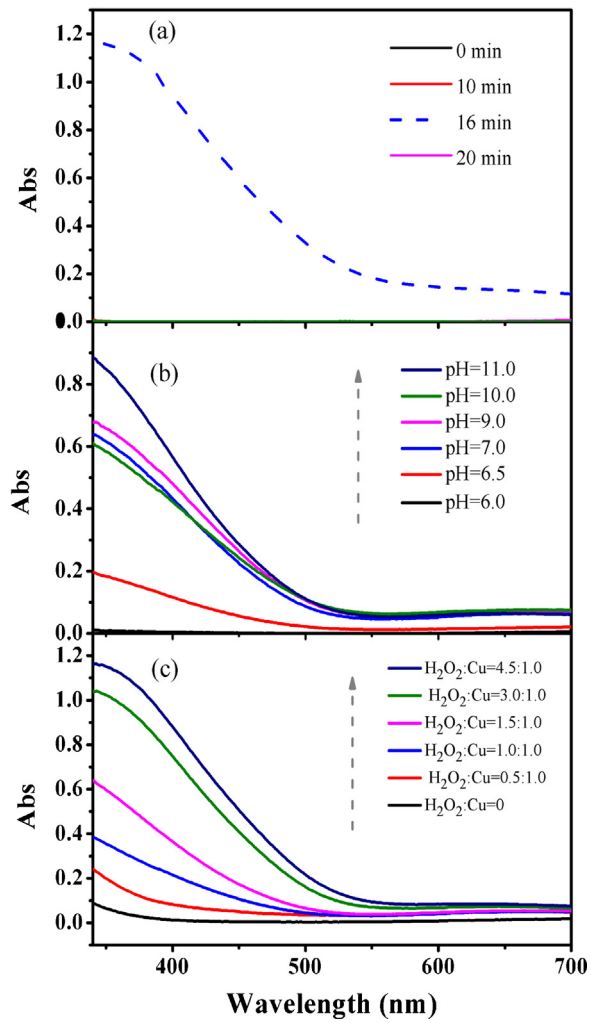

Fig. 7. (a) change of absorbance spectra during process of $Cu(CN)_3^{2-}$ oxidation by H_2O_2 ($Cu(CN)_3^{2-}$: 1.0 mM, CN^-: 1.0 mM, H_2O_2: 12.0 mM, pH: 11, *T*: 25 °C); (b) change of absorbance spectra with pH values in the reaction of Cu^{2+} with H_2O_2 (Cu^{2+}: 1.0 mM, H_2O_2: 3.0 mM, pH: 11, *T*: 25 °C); (c) change of absorbance spectra with H_2O_2 dose in the reaction of Cu^{2+} with H_2O_2 (Cu^{2+}: 1.0 mM, pH: 11, *T*: 25 °C).

the increase of H_2O_2 concentration (Fig. 7(c)). The superoxo-cupric complex ($HO_2Cu(OH)_2^-$) was identified as the key species in the reaction of H_2O_2 with Cu^{2+} in strongly alkaline medium [40]. The $HO_2Cu(OH)_2^-$ was unstable, which was further decomposed into Cu^+ species and superoxide radical in unimolecular [40]. The superoxide radical served as a precursor for O_2. It is concluded that the H_2O_2 was decomposed via such pathway.

3.4. A proposed process of $Cu(CN)_3^{2-}$ destruction by H_2O_2

On the basis of the above results, a reaction process of $Cu(CN)_3^{2-}$ with H_2O_2 is proposed. As shown in Scheme 1, H_2O_2 oxidizes $Cu(CN)_3^{2-}$ to $Cu(CN)_2^-$ with the formation of cyanate and H_2O (Eq. (1)) firstly. The oxidization of complex cyanide species is faster than oxidation of free cyanide due to its higher reactivity activity with H_2O_2. Thus, the $Cu(CN)_2^-$ reacts with excess free cyanide to form $Cu(CN)_3^{2-}$ immediately (Eq. (2)). The oxidation and re-formation of $Cu(CN)_3^{2-}$ proceed simultaneously until no free cyanide. The further oxidation of ligands (CN^-) leads to progressive destruction of $Cu(CN)_2^-$, followed by release of Cu^+ (Eq. (3)). The released Cu^+ reacts with H_2O_2 to form Cu^{2+} and •OH (Eq. (4)). It can be considered as a Fenton-like reaction. The formation of superoxo-cupric complex ($HO_2Cu(OH)_2^-$) between Cu^{2+} species and H_2O_2 is

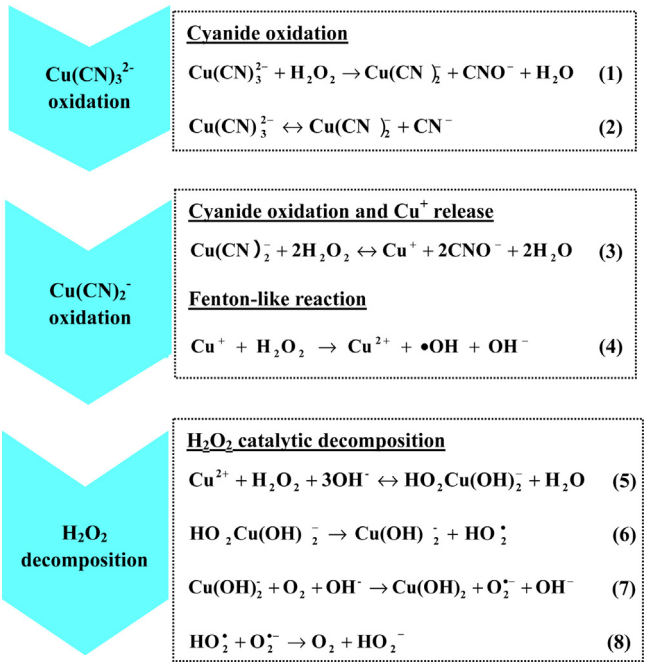

Scheme 1. A proposed reaction process of $Cu(CN)_3^{2-}$ with H_2O_2.

verified afterward in alkaline conditions (Eq. (5)). The $HO_2Cu(OH)_2^-$ is further decomposed into Cu^+ species and superoxide radical ($O_2\bullet^-$) in unimolecular due to its low stability (Eq. (6)). The Cu^+ is subsequently oxidized to Cu^{2+} by $O_2\bullet^-$ or O_2 (Eq. (7)). The catalytic cycle between Cu^+/Cu^{2+} species is then propagated by the continuous oxidation with H_2O_2 and reactive oxygen species. The decomposition of H_2O_2 give off O_2. The $O_2\bullet^-$ serves as a precursor for O_2 formation (Eq. (8)).

4. Conclusions

In this work, we investigated the reaction of $Cu(CN)_3^{2-}$ with H_2O_2 in water at pH 11.0. The destruction of $Cu(CN)_3^{2-}$ was investigated though stoichiometry study. In the course of $Cu(CN)_3^{2-}$ destruction, the decomposition of H_2O_2 and its products were examined. At the same time, the species of copper were also identified using various spectra (XPS, XRD and UV–vis). On the basis of these results, a reaction process of $Cu(CN)_3^{2-}$ with H_2O_2 in water at pH 11.0 was proposed. It was found that:

(1) The $Cu(CN)_3^{2-}$ was destroyed progressively by H_2O_2, resulting from oxidation of cyanide to cyanate. The $Cu(CN)_3^{2-}$ could be destructed completely with the consumption of a large amount of H_2O_2.
(2) The reaction of Cu^+ with H_2O_2 proceeded via a Fenton-like reaction. The catalytic reaction did not occurred until the Cu^+ was liberated from the complexes.
(3) The H_2O_2 was decomposed into O_2 by the catalysis of Cu^+/Cu^{2+} species under alkaline conditions, which reduced the utilization of H_2O_2 for cyanide oxidation.

Acknowledgments

This work was supported by the Major Program of the National Natural Science Foundation of China (No. 51290282) and National Natural Science Foundation of China (Nos. 51221892, 51222802).

Appendix A. Supplementary data

Supplementary data associated with this article can be found, in the online version, at http://dx.doi.org/10.1016/j.apcatb.2014.04.010.

References

[1] M.Y. Li, Q.X. Zeng, Z.Q. Cao, Y.R. Sun, Adv. Mater. Res. 476 (2012) 1847–1850.
[2] X. Dai, A. Simons, P. Breuer, Miner. Eng. 25 (2012) 1–13.
[3] F.R. Pombo, A.J.B. Dutra, Environ. Prog. Sustain. Energy 32 (2013) 52–59.
[4] Ü.B. Öğütveren, E. Törü, S. Koparal, Water Res. 33 (1999) 1851–1856.
[5] S.C. Cheng, M. Gattrell, T. Guena, B. MacDougall, Electrochim. Acta 47 (2002) 3245–3256.
[6] M. Hijosa-Valsero, R. Molina, H. Schikora, M. Müller, J.M. Bayona, Water Res. 47 (2013) 1701–1707.
[7] R.R. Dash, C.A. Gaur, C. Balomajumder, J. Hazard. Mater. 163 (2009) 1–11.
[8] D. Novak, I.H. Franke-Whittle, E.T. Pirc, V. Jerman, H. Insam, R.M. Logar, B. Stres, Water Res. 47 (2013) 3644–3653.
[9] M.A. Barakat, Y.T. Chen, C.P. Huang, Appl. Catal., B: Environ. 53 (2004) 13–20.
[10] M.J. López-Muñoz, J. Aguado, R. van Grieken, J. Marugán, Appl. Catal., B: Environ. 86 (2009) 53–62.
[11] P. Oulego, A. Laca, M. Diaz, Environ. Sci. Technol. 47 (2012) 1542–1549.
[12] V.K. Sharma, W. Rivera, J.O. Smith, Environ. Sci. Technol. 32 (1998) 2608–2613.
[13] V.K. Sharma, C.R. Burnett, R.A. Yngard, D.E. Cabelli, Environ. Sci. Technol. 39 (2005) 3849–3854.
[14] J.Q. Jiang, B. Lloyd, Water Res. 36 (2002) 1397–1408.
[15] J.A. Zeevalkink, D.C. Visser, P. Arnoldy, C. Boelhouwer, Water Res. 14 (1980) 1375–1385.
[16] G.E. Eden, B.L. Hampson, A.B. Wheatland, J. Chem. Technol. Biotechnol. 69 (1950) 244–249.
[17] X. Yang, C. Shang, Environ. Sci. Technol. 38 (2004) 4995–5001.
[18] R.R. Dash, C. Balomajumder, A. Kumar, Chem. Eng. J. 146 (2009) 408–413.
[19] G. Moussavi, F. Majidi, M. Farzadkia, Desalination 280 (2011) 127–133.
[20] K. Osathaphan, T. Boonpitak, T. Laopirojana, V.K. Sharma, Water, Air, Soil Pollut. 194 (2008) 179–183.
[21] M. Sarla, M. Pandit, D.K. Tyagi, J.C. Kapoor, J. Hazard. Mater. 116 (2004) 49–56.
[22] M. Kitis, E. Karakaya, N.O. Yigit, G. Civelekoglu, A. Akcil, Water Res. 39 (2005) 1652–1662.
[23] A.R. Yeddou, B. Nadjemi, F. Halet, A. Ould-Dris, J. Belkouch, Miner. Eng. 24 (2011) 788–793.
[24] J.K. Beattie, G.A. Polyblank, Aust. J. Chem. 48 (1995) 861–868.
[25] M.K. Eberhardt, G. Ramirez, E. Ayala, J. Org. Chem. 54 (1989) 5922–5926.
[26] M. Masarwa, H. Cohen, D. Meyerstein, D.L. Andreja, H. Bakac, J.H. Espenson, J. Am. Chem. Soc. 110 (1988) 4293–4297.
[27] A.N. Pham, G. Xing, C.J. Miller, T.D. Waite, J. Catal. 301 (2013) 54–64.
[28] J.W. Moffett, R.G. Zika, Environ. Sci. Technol. 21 (1987) 804–810.
[29] G.C. Lukey, J.S. van Deventer, S.T. Huntington, R.L. Chowdhury, D.C. Shallcross, Hydrometallurgy 53 (1999) 233–244.
[30] H. Deveci, İ. Alp, J. Hazard. Mater. 166 (2009) 1362–1366.
[31] Z.M. Qiang, J.H. Chang, C.P. Huang, Water Res. 36 (2002) 86–94.
[32] APHA, AWWA, WEF, Standard Methods for the Examination of Water and Wastewater, 21th ed., APHA, Washington, DC, 2005.
[33] G.M. Eisenberg, Ind. Eng. Chem. 15 (1943) 327–328.
[34] M.G. Steiner, C.F. Babbs, Arch. Biochem. Biophys. 278 (1990) 478–481.
[35] C.F. Babbs, M.J. Gale, Anal. Biochem. 163 (1987) 67–73.
[36] V.M. Rayón, P. Redondo, H. Valdés, C. Barrientos, A. Largo, J. Phys. Chem. A 111 (2007) 6334–6344.
[37] Z.H. Ai, P. Yang, X.H. Lu, Chemosphere 60 (2005) 824–827.
[38] Y.L. Nie, C. Hu, J.H. Qu, X. Zhao, Appl. Catal., B: Environ. 87 (2009) 30–36.
[39] L.L. Zhang, Y.L. Nie, C. Hu, J.H. Qu, Appl. Catal., B: Environ. 12 (2012) 418–424.
[40] Y. Luo, M. Orbfin, K. Kustin, I.R. Epstein, J. Am. Chem. Soc. 111 (1989) 4541–4548.